PROCEEDINGS

2020 7th International Congress on Energy Fluxes and Radiation Effects (EFRE)

Tomsk, Russia, September 14 – 26, 2020

SPONSORED BY

IEEE Nuclear and Plasma Sciences Society

Institute of High Current Electronics of the Siberian Branch of the Russian Academy of Sciences

National Research Tomsk Polytechnic University

Tomsk Scientific Center of the Siberian Branch of the Russian Academy of Sciences

Chairman

Nikolay Ratakhin
Institute of High Current Electronics, Tomsk, Russia

Co-Chairman

Andrey Yakovlev
National Research Tomsk Polytechnic University, Tomsk, Russia

Alexey Markov
Tomsk Scientific Center SB RAS, Tomsk, Russia

Program Chairman

Alexander Batrakov
Institute of High Current Electronics, Tomsk, Russia

Program Co-Chairman

Edl Schamiloglu
University of New Mexico, Albuquerque, USA

Mechanical Properties of Weld Joints of High-Strength Steel under Dynamic Loading

Vladimir V. Skripnyak
Institute of Strength Physics and Material Sience SB RAS,
2/4 Akademichesky Ave., 634055,
Tomsk, Russia
National Research Tomsk State University
36 Lenin Ave., 634050,
Tomsk, Russia
skrp2012@yandex.ru

Alexander Kozulin
Institute of Strength Physics and Material Sience SB RAS,
2/4 Akademichesky Ave., 634055,
Tomsk, Russia
National Research Tomsk State University
36 Lenin Ave., 634050,
Tomsk, Russia
skrp2012@yandex.ru
kozulyn@ftf.tsu.ru

Vladimir A. Skripnyak
National Research Tomsk State University
36 Lenin Ave., 634050,
Tomsk, Russia
skrp2006@yandex.ru

Anna Bevz
National Research Tomsk State University
36 Lenin Ave., 634050,
Tomsk, Russia
skrp2012@yandex.ru
anna.bevz.94@mail.ru

Evgeniya G. Skripnyak
National Research Tomsk State University
36 Lenin Ave., 634050,
Tomsk, Russia
skrp2012@yandex.ru
skrp @ftf.tsu.ru

***Abstract*— The paper represents a computational model for predicting the mechanical behavior of welded joints in steel constructions under dynamic load, taking into account the change in the properties of the steel in the welding zone. Plastic deformation localization and formation of cracks in welded joints subjected to tensile loading have been studied numerically. Numerical modeling confirms that the model proposed in the work can predict the strength and mechanical behavior of welded joints in steel constructions in a wide range of strain rates, taking into account the phase and granular structure in the weld area. The results confirm that residual stresses of ~ 100–150 MPa do not significantly affect the formation of the fracture zone in arc welded joints of 09G2S steel subjected to dynamic loading. Fracture of considered welded joints exhibits ductile behavior at initial temperature of 295K and high strain rates. The results have shown that mesoscopic cracks nucleate in the heat-affected zone at effective strains above 12%.**

Keywords*— *silicon-manganese steel, welding joints, dynamic tensile strength.

I. INTRODUCTION

Welded joints of elements made of high-strength steels are used in critical steel structures of pipeline systems, machines, and large industrial and public buildings, bridges. To assess the strength of these structures under shock and explosive load, which may occur as the result of terrorist attacks and accidental explosions, numerical modeling techniques that take into account the microstructure of welded joints and welding technology are considered.

Hea et al. showed that the strength of welded joints of high-strength steel structures is determined by damage to the welds and the zone of their thermal influence at a high strain rate of explosive loads [1].

The peculiarity of predicting the dynamic strength of welded joints in steel constructions is due to the fact that the material of the welded joint is more sensitive to the strain rate compared to welded steels [2]. As a rule, the yield strength of the weld material at high strain rates increases significantly compared with the static loading.

The need of using the fracture criterion of welded joints, taking into account the relationship between critical plastic strain and the stress triaxiality for individual welding zones was experimentally proved by Paveebunvipak et al. [3].

Modern methods for assessing the mechanical properties of welded joints take into account loading conditions and the intensity of residual stresses in the weld zone [4-6]. Computational models taking into account the effect of the structure of steels in the welded joint zone on the deformation and fracture of welded joints are currently under development.

However, the effect of the mechanical heterogeneity of materials in the welded zone on fracture of welded joints is not included directly in these parameters and needs to be studied.

The improvement of methods for assessing the dynamic strength of welded structures is related to taking into account the microstructure of the material in the weld zone.

This work was supported by the Russian Science Foundation (RSF), grant No. 16-19-10010.

978-1-7281-2686-9/20/$31.00 ©2020 IEEE

The mechanical heterogeneity of the microstructure can lead to a significant localization of deformations in the welding zone under dynamic loads. As a result of plastic deformation of the welded joint, cracks can nucleate and propagate in it.

The aim of this work is to study the dynamics of fracture and deformation at high strain rates of welded joints of thick-walled steel panels using a model that takes into account the inhomogeneous structure in the welding zone and changes the mechanical properties at the mesoscale level.

II. Simulation Of The Welded Joints Of Steel Under Quasistatic And Dynamic Loading

The deformation and fracture of a welded joint of 6 mm thick plates of 09G2S steel, created by pulsed CO_2 arc welding, were studied under tension under conditions of quasi-static and dynamic loading. Using optical microscopy, it was found that in the cross section of the welded joint, 7 local regions can be distinguished that are similar in phase morphology and grain structures. The arrangement of regions in the weld zone is shown in Fig. 1.

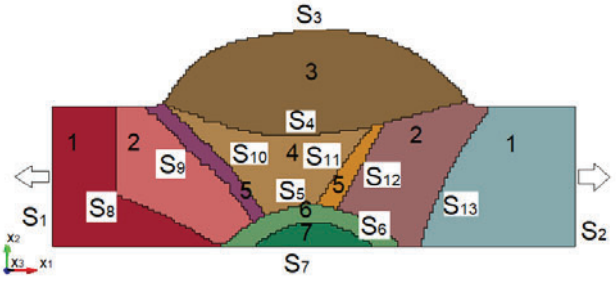

Fig. 1. Scheme of boundary conditions of a loaded welded joint of steel plates.

The base material is marked as 1. Region 2 corresponds to the heat affected zone (HAZ). Microstructures of 3, 4, 7 regions of welded zone depend on the chemical composition of the electrode material. For silicon-manganese steel, these regions have quenching structures. Region 5 is a fusion zone of the base material and the electrode material. The measured microhardness confirmed the differences in the mechanical properties of these local regions. The yield strengths (Fig. 2) and tensile strengths of the material in local areas were estimated by the microhardness value using the phenomenological relations obtained by Zhu et al. [6]. These data were used to determine the numerical values of the parameters of the governing equation given in Table I. The computational model uses the theoretical basis of continuum damage mechanics [7]. Mechanical behavior of the volume with a welded joints under tension was described by a system of conservation equations (mass, momentum and energy), a kinematic equation, and a constitutive equation.

Computer simulations of deformation and fracture processes were performed using licensed software ANSYS 14.5, which is the part of the software LS-DYNA. The calculations were carried out with solvers using a finite difference scheme of second-order accuracy.

The initial and boundary conditions were added to the system of equations. Initial condition corresponded to the state of the material in the uniform temperature field T_0:

$$\rho\big|_{t=0} = \rho_0,\ \varepsilon_{ij}\big|_{t=0} = 0,\ \sigma_{ij}\big|_{t=0} = 0,\ T\big|_{t=0} = T_0, \tag{1}$$

where t is time, ρ is a mass density, ρ_0 is the initial mass density, σ_{ij} are the components of stress tensor, ε_{ij} are components of the strain tensor, T is the temperature, T0 is the initial temperature.

The boundary conditions (2) correspond to the conditions of loading of a 3D welded joint of plates. The scheme for setting the boundary conditions is shown in Fig. 1.

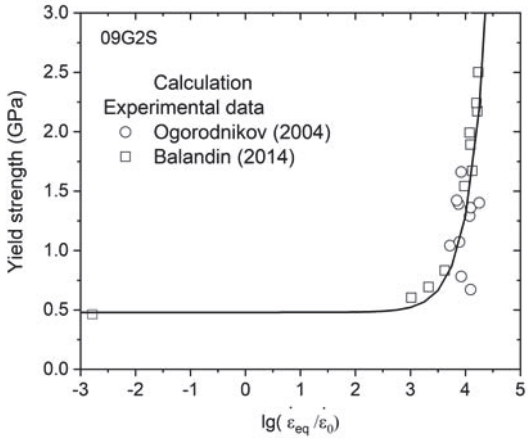

Fig. 2. Yield strength versus logarithm of normalized strain rate.

The 3D structured volume of the welded joint of steel plates with dimensions of 22 mm × 6 mm × 5.9 mm was numerically simulated under axial tension with a constant strain rates from 1 to 9000 s^{-1}. The volume of material in the weld zone consists of interconnected mesoscopic volumes with a different phase structure and grain sizes that differ from the material joined by welding. The surfaces of the mesoscopic volumes of the material S_k (k = 4 ... 13) in the section of the volume are shown in Fig. 1.

$$\begin{aligned} &u_1\big|_{S_1} = 0,\ u_1\big|_{S_2} = V_0,\ \sigma_{ij}\big|_{S_3} = 0,\ \sigma_{ij}\big|_{S_7} = 0, \\ &\sigma_{ij}(x_k + \delta) = \sigma_{ij}(x_k - \delta)\big|_{S4 \cup S_5 \cup S_6 \cup S_8 \cup S_9 \cup S_{10} \cup S_{11} \cup S_{12} \cup S_{13}} \end{aligned} \tag{2}$$

where $u_i \,|\, S_j$ are the components of the particles velocity vector on the surface S_j, V_0 is the tensile velocity, σ_{ij} are the components of the stress tensor.

Plastic flow was described within the Prandtl–Reuss theory by the von Mises criterion. The flow stress of silicon-manganese steel under loading has been described using a modification of the Zerilli–Armstrong model [8–9]:

$$\sigma_s^{(m)}(\varepsilon_{eq}^p, \dot{\varepsilon}_{eq}, T) = C_0 + k_h d_g^{-1/2} + [\mu(T)/\mu(295\,K)]\times \times\{C_5 + (\varepsilon_{eq}^p)^{0.5} C_2 \exp[(-C_3 + C_4 \ln(\dot{\varepsilon}_{eq}/\dot{\varepsilon}_0))T]\}, \quad (3)$$

where $\varepsilon_{eq}^p = [(2/3)\varepsilon_{ij}^p \varepsilon_{ij}^p]^{1/2}$, $\dot{\varepsilon}_{eq} = [(2/3)\dot{\varepsilon}_{ij}\dot{\varepsilon}_{ij}]^{1/2}$, $\dot{\varepsilon}_0 = 1.0\,s^{-1}$, C_0, C_2, C_3, C_4, C_5, k_h, n are the material constants, T is the absolute temperature, d_g is the averaged grain size.

The coefficient k_h for silicon-manganese steel was equal to k_h = 391 MPa μm$^{1/2}$ [10, 11]. Constants of the Zerilli-Armstrong constitutive equation for 09G2S silicon-manganese steel are C_5 = 0 GPa. Constants C_2, C_3, C_4, and $C_0+k_h d_g^{-1/2}$ are shown in Table I.

TABLE I. CONSTANTS OF MODEL FOR REGIONS OF WELDED ZONE.

Constants	$C_0+k_h d_g^{-1/2}$, GPa	C_2, GPa	C_3, K^{-1}	C_4K^{-1}
region 1	0.275	1.05	0.0018	0.00028
region 2	0.35	0.62	0.0018	0.00028
region 3	0.48	0.47	0.00162	0.000252
region 4	0.35	0.62	0.0018	0.00028
region 5	0.57	0.38	0.00162	0.000252
region 6	0.86	0.23	0.00162	0.000252
region 7	0.7	0.28	0.00162	0.000252

The calculated stress-strain curves in comparison with experimental data [12–15] for materials in areas 1–7 in the weld zone of 09G2S steel are shown in Fig. 3. Note that the base ferritic-pearlitic steel and the steel in the heat affected zone have close parameters of the strain rate sensitivity of the yield stress. For areas with a bainitic microstructure (6) and (7) as well as the diffusion zone of welded steel with electrode material, the strain rate sensitivity of the yield stress is lower than that of base steel.

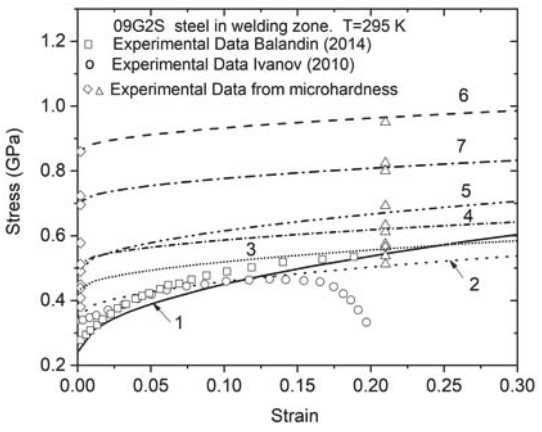

Fig. 3. Stress-strain curves for regions in the weld zone of 09G2S steel.

Local temperature in the material particles of a deformed body was calculated by relation:

$$T = T_0 + (0.9/\rho C_p)\int_0^{\varepsilon_{eq}^p} \sigma_{eq}\, d\varepsilon_{eq}^p, \quad (4)$$

where T_0 =295 K is the initial temperature, ρ =7.832 g/cm^3 is mass density of alloy, C_p= 494 J/kg K is the specific heat of the 09G2S steel, E= 203 GPa is the Young's modulus, the Poisson's ratio ν =0.3 [12-17].

$$\mu = \mu_0 (1 - k_\mu T), \quad (5)$$

where μ is the shear modulus, T is temperature, μ_0 = 84.7GPa, k_μ = 0.000276.

The GISSMO model was used for the damage and fracture analysis of silicon-manganese steel under tension [18]. The yield criterion has a form:

$$\sigma_s = \sigma_s^{(m)}[1 - (\frac{D - D_c}{1 - D_c})^F], \quad (6)$$

where σ_s is the yield stress of damaged medium, $\sigma_s^{(m)}$ is the yield stress of condensed phase of material, D is the damage parameter, D_c is the critical values of damage, F is the fading exponent.

A strong coupling between plastic strain and damage parameter is introduced by relation:

$$D = (\varepsilon_{eq}^p / \varepsilon_f)^q, \quad (7)$$

where ε_f, q are constants of material.

The final stage of ductile fracture is the coalescence of damage into the fracture zone. This causes softening of the material and the accelerated growth of the damage parameter D until the local fracture of the material particle.

The model of ductile fracture requires values of 4 parameters. The model parameters for silicon-manganese steel were determined using numerical simulation of experiments on the tension of silicon-manganese steel samples in a wide strain rates. The numerical values of model parameters are given in Table II.

TABLE II. PARAMETERS OF THE GISSMO MODEL FOR 09G2S STEEL.

Parameter	D_c	F	ε_f	q
09G2S steel	0.0	2	0.3	2

The model was used for simulation of welded joints of 6 mm 09G2S steel plates under tension at velocity 20 m/s and 200 m/s.

III. RESULTS

Fig. 4 shows calculated equivalent stress in a section of welded zone under tension at 200 m/s.

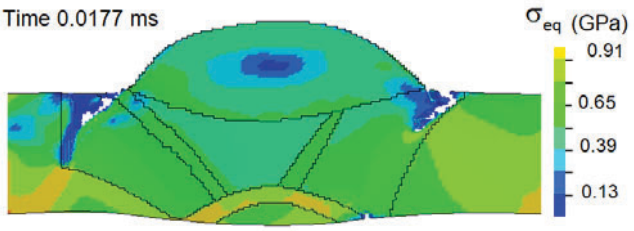

Fig. 4. Equivalent stress in welded joint steel plates under tension at 200 m/s.

Increasing the cross-sectional area of the structure that subjected to load can be caused by the presence of additionally deposited steel in the welding zone (Fig. 1). As a result, the effective stresses in the welding zone are slightly lower than in the material at a distance from the welding area. The parameter of stress triaxiality changes at the weld zone boundary during weld joint deformation, as shown in Fig. 5.

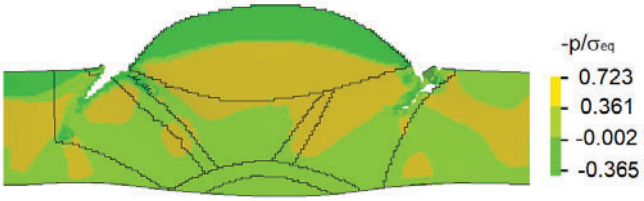

Fig. 5. The stress triaxiality factor in damaged welded joint steel plates under tension at 200 m/s.

The heterogeneity of the field of equivalent stresses and the stress triaxiality parameter causes the localization of plastic deformation near the weld boundary. Fig. 6 shows the field of the equivalent plastic strain in the section of welded joint steel plates under tension at the velocity of 200 m/s.

The heterogeneity of the field of equivalent stresses and the parameter of the stress triaxiality factor causes the localization of plastic deformation near the weld boundary. Fig. 6a shows the equivalent plastic strain before damage nucleation, Fig.6b shows the evolution of the equivalent plastic strain at the beginning of cracks formation. An increase in the strain rate causes localization of plastic deformation at lower strain values.

Fig. 7 shows the distribution of damage parameter in the welding zone of steel plates under tension at strain rate of 9000 s^{-1}.

IV. Discussion

The simulation results in Fig. 7 demonstrate that crack formation affect the stress state triaxiality in the heat affected zone, the plastic flow stress, and evolution of damage in the silicon-manganese steel at high strain rates. The introduction of the stress triaxiality in the plastic flow model is important for prediction of damage evolution under deformation especially at high strain rates.

Damage kinetics in silicon-manganese steel is related to the macroscale plastic instability.

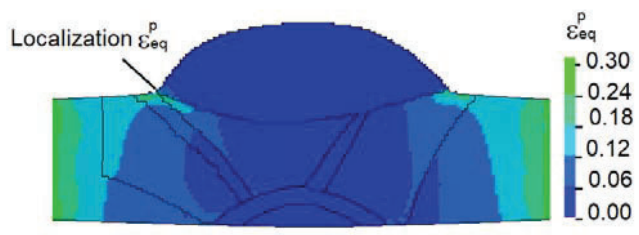

(a)

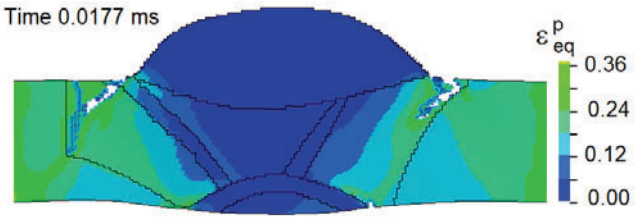

(b)

Fig. 6. Equivalent plastic deformation in the weld zone under tension at a velocity of 200 m/s.

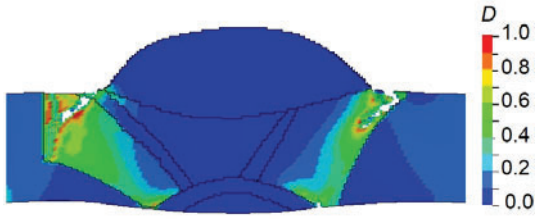

Fig. 7. Damage and crack formation of welded joint steel plates under tension at the velocity of 200 m/s.

Fig. 8 shows the calculated curve of effective stresses and strains obtained for high-speed tension of a welded joint.

These results confirm that, under dynamic loading of welded joints of 09G2S steel, obtained by arc welding in protective CO_2, the residual stresses (~ 100…150 MPa [19]) do not significantly affect the formation of the fracture zone. The obtained results confirm the possibility of expanding the choice of technological modes for arc welding of constructions made of manganese-silicon steels subjected to dynamic loading.

A sharp drop in stress at effective strains of ~ 2.5% is associated with the development of plastic strains in the weld zone. At the initial stage of loading, the metal in the weld zone experiences lower tensile stresses compared to the base metal due to the distribution of forces over a large area due to the presence of deposited metal (region 3 in Fig. 1).

Under intense dynamic loading, the ductile fracture of the welded joints occurs at temperatures of ~ 295 K. Note that at effective strains exceeding 12% in the welded joint zone, plastic deformation is localized in the heat-affected zone and mesoscopic cracks begin to develop.

The calculated configuration of the crack is in good agreement with the experimental data in terms of location, shape and length of cracks [20].

Thus presented experimental and theoretical results demonstrate the importance of an adequate description of the processes of instability of deformation in silicon-manganese steel.

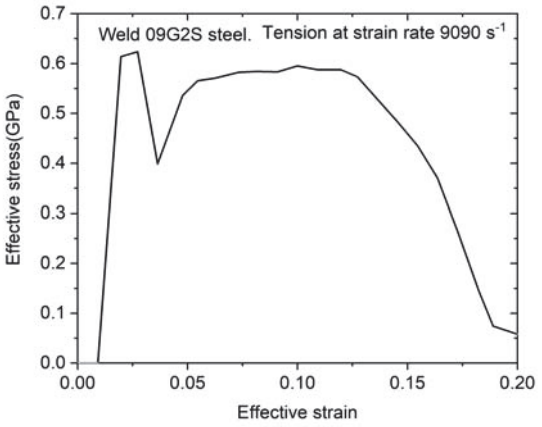

Fig. 8. Effective tensile stress in the welded joint of 09G2S steel plates at a strain rate of ~ 9.09 10^3 s^{-1}.

V. Conclusion

Presented results demonstrate the importance of an adequate description of the processes of instability of plastic deformation in welded joints of structural elements made of silicon-manganese steel under dynamic loading.

The areas in welded joints in which the plastic deformation localized and cracks occurred under dynamic tension were determined.

A physical mathematical model is presented for predicting the mechanical behavior of welded steel joints under dynamic loads, taking into account the change in the properties of the material in the welding zone.

The results of numerical modeling confirm that the model proposed in the work can predict the strength and mechanical behavior of welded steel joints in a wide range of strain rates.

The fracture of welded joins at high strain rates depends on relationships between critical plastic strains and stress triaxiality for the individual weld zones.

Acknowledgment

This work was supported by the Russian Science Foundation (RSF), grant No. 16-19-10010. The authors are grateful for the support of this research.

References

[1] Z. Hea, X. Liu, J. Yeb, L. Yanc, "Experimental study on welding dynamic mechanical properties of Q460JSC and HQ600 high strength steel at high strain rate," *MMAEE-2019 IOP Conf. Series: Mater. Sci. and Eng.*, vol. 677, Art. no. 022020, December 2019.

[2] B.Wang, G. X. Lu, "Dynamic strength of steel welds under high strain rate loading," *Advanc. Mater. Res.*, vol.9, pp.87–92, September 2005.

[3] K. Paveebunvipak, V. Uthaisangsuk, "Microstructure based modeling of deformation and failure of spot-welded advanced high strength steels sheets," *Materials & Design*, vol. 160, pp. 731–751, December 2018.

[4] S. S. Miller, "Computer simulation of the submerged arc welding process on the basis of self-consistent physicomathematical model," *Int. J. Eng. Res. Tech.*, vol. 11, pp. 1837–1850, December 2018

[5] D. Anderson, C. Butcher, N.Pathak, M.J. Worswik, "Failure parameter identification and validation for a dual-phase 780 steel sheet," *Int. J. Solids and Struct.*, vol. 124, pp. 89–107, October 2017.

[6] M.-L. Zhu, F.-Z. Xuan, "Correlation between microstructure, hardness and strength in HAZ of dissimilar welds of rotor steels," *Materials Science and Engineering: A*, vol. 527, pp. 4035–4042, 2010.

[7] V. A. Skripnyak, N. V. Skripnyak, E. G. Skripnyak, V. V. Skripnyak, "Influence of grain size distribution on the mechanical behavior of light alloys in wide range of strain rates," *AIP Conf. Proc.*, vol. 1793, Art. no. 110001, 2017.

[8] R. W. Armstrong, F. J. Zerilli, "Dislocation mechanics aspects of plastic instability and shear banding," *Mech. Mater.,* vol. 17, pp. 319–327, October 1994.

[9] A. He, G.L. Xie, H. L. Zhang, X. T. Wang, "A modified Zerilli–Armstrong constitutive model to predict hot deformation behaviour of 20CrMo alloy steel," *Materials & Design.*, vol.56, pp.122–127, November 2014.

[10] F. Jiang, T. Masumura, T. Tsuchiyama, S.Takaki, "Effect of substitutional element addition on Hall-Petch relationship in interstitial free ferritic steels," *ISIJ International*, vol. 5, pp. 1929–1931, September 2019.

[11] M. Schneider, F. Werner, D. Langenkämper, C. Reinhart, G. Laplanche, "Effect of temperature and texture on hall–petch strengthening by grain and annealing twin boundaries in the MnFeNi medium-entropy alloy," *Metals*, vol. 9, pp.84. September 2019.

[12] V. V. Balandin, V. V. Balandin, A. M. Bragov, L. A. Igumnov, A. Yu. Konstantinov, A. K.Lomunov, "High-speed deformation and fracture of 09G2S steel," *Solid Mechanics*, no. 6, p.78–85, November 2014. (in Russian)

[13] A. M. Ivanov, E. S. Lukin, N. D. Petrova, S. S. Vashenko, "Deformation and direction of the structural steel subjected to severe plastic deformation," *Rev. Adv. Mater. Sci.*, vol. 25, pp. 203–208, January 2010.

[14] V. A. Ogorodnikov, E. Yu. Borovkova, and S. V. Erunov,"Strength of Some Grades of Steel and ArmcoIron under Shock Compression and Rarefaction at Pressures of 2–200GPa," *Comb. Expl. Shock Waves*, vol. 40, pp.597–604, September 2004.

[15] M. Fujita, K. Kuki, "An evaluation of mechanical properties with the hardness of building steel structural members for reuse by NDT," Metals, vol. 6, Art. no. 2472016, October 2016.

[16] M. Ledbetter, M. W. Austin, "Elastic constant versus temperature behavior of three hardened maraging steels," *Materials Science and Engineering*, vol. 72, pp.65–69, October 1985.

[17] Y. Bao, H. Zhang, M. Ahmadi, M. A. Karim, H. F. Wu, "Measurements of Young's and shear moduli of rail steel at elevated temperatures," *Ultrasonics*, vol. 54, pp. 867–873, March 2014.

[18] Y. Xiao, Y. Hu, "An extended iterative identification method for the GISSMO Model," *Metals*, vol. 9, p. 568*,* May 2019.

[19] Y. N. Sarayev, V. P. Bezborodov, A. A. Grigoryeva, N. I. Golikov, V. V. Dmitriev, I. I. Sannikov, "Distribution of residual stresses in welded joints in 09G2S steel produced by adaptive pulsed-arc welding," *Welding International*,vol. 29, pp. 131–134, February 2014.

[20] M. Kocak, "Structural integrity of welded structures: Process – Property – Performance (3P) Relationship," in *Proc. of 63rd Annual Assembly & International Conference of the International Institute of Welding* 11–17 July 2010, Istanbul, Turkey, pp.1–19, January 2010.